Pb Nanoprecipitates in Al: Magic-Shape Effects due to Elastic Strain

J. C. Hamilton,[1] F. Léonard,[1] E. Johnson,[2] and U. Dahmen[3]

[1]*Sandia National Laboratories, Livermore, California, USA*

[2]*Nano Science Center, Niels Bohr Institute, University of Copenhagen, Copenhagen, Denmark and Department of Materials Research, Riso National Laboratory, Roskilde, Denmark*

[3]*National Center for Electron Microscopy, Lawrence Berkeley National Laboratory, Berkeley, California, USA*

(Received 27 November 2006; published 5 June 2007)

We present a theory for size-dependent shapes of Pb nanoprecipitates in Al, introducing the concept of "magic shapes," i.e., shapes having near-zero homogeneous elastic strains. Our quantitative atomistic calculations of edge energies show their effect on precipitate shape to be negligible, thus it appears that shapes must be due to the combined effect of strain and interface energies. By employing an algorithm for generating magic shapes, we replicate the experimental observations by selecting magic-shape precipitates with interfacial energies less than a cutoff value.

DOI: 10.1103/PhysRevLett.98.236102 PACS numbers: 68.35.−p, 61.46.Bc, 61.72.Qq, 62.20.Dc

A major goal of nanoscience is to understand and control the properties of functional nanostructures, including, for example, catalyst particles, quantum dots on surfaces, and inclusions in alloys. Such properties are often determined by the nanostructure shape. The Wulff construction, based on minimization of interfacial energy subject to a constraint of constant volume, predicts that the cluster shape will be independent of cluster size. Experimentally, however, changes in cluster shapes are often observed as cluster sizes approach the nanoscale. Conventionally such size-dependent shape effects are attributed to the increasing contribution of edge energies relative to interfacial energies at small size. For example, edge energies are included in theories for the shapes of snow crystals [1], discussions of surface faceting [2], theories for the shapes of strained Ge pyramids grown on a surface [3], and discussions of Pb inclusions in bulk Al [4]. Until very recently [5,6], no atomistic calculations of edge energies had been published.

Here we present a theoretical examination of size-dependent shapes observed for Pb nanoprecipitates in Al [4,7]. Using the embedded atom method (EAM) with potentials from Landa and co-workers [8], quantitative calculations of the total precipitate energies and relevant edge energies were performed. We find the effect of edge energies on precipitate shape to be negligible for all sizes and conclude that observed size-dependent shape effects must be explained by the minimization of interfacial energy and strain energy. We present an algorithm for generating precipitate shapes with very small homogeneous strain energies and use the term "magic shapes" to describe these special precipitate shapes. The minimization of precipitate interfacial energies subject to the magic-shape constraint accounts for the observed size-dependent shape effects.

Figure 1 summarizes the experimental TEM observations for Pb precipitates formed by ion implantation and annealing [7]. A few of the smallest precipitates are octahedral, bounded by {111}-type Pb/Al interfaces. The largest precipitates are approximately tetrakaidecahedral, bounded by {111}- and {100}-type Pb/Al interfaces (see upper right inset of Fig. 1). The plotted aspect ratio is $C/\bar{A} = 2C/(A_1 + A_2)$ where C is the spacing between a pair of {100}-type interfaces, and A_1 and A_2 are the spacings between the two pairs of {111}-type interfaces. EAM calculations for Pb/Al interfacial free energies have previously been reported [9] giving $\gamma_{100} = 48.44$ meV/Å^2 and $\gamma_{111} = 41.44$ meV/Å^2 at $T = 400$ K (in the vicinity of the experimental annealing temperature). The predicted aspect ratio at 400 K from the Wulff construction is $C/A = \gamma_{100}/g_{111} = 1.165$. For larger precipitates, the measured aspect ratio is close to this value; however, as seen in Fig. 1, smaller precipitates behave quite differently, and exhibit a wide range of aspect ratios.

To understand these shape effects, we calculated precipitate energies for octahedral, tetrakaidecahedral, and cuboctahedral Pb precipitates inserted into similarly shaped voids in a block of Al with periodic boundary conditions. The sizes and shapes of the Pb precipitates and the Al voids were selected to obtain relatively small homogeneous elastic strains. Figure 2 compares the calculated precipitate energies for the different shapes over a range of precipitate sizes. The x axis is $N_{\mathrm{Pb}}^{1/3}$ which, for a given shape, is proportional to the edge length, thus allowing comparison of energies for precipitates with similar volumes (i.e., similar $N_{\mathrm{Pb}}^{1/3}$). For this 0 K calculation, the Wulff construction predicts $C/A = 1.31$, based on $T = 0$ K EAM interface energies, $\gamma_{100} = 36.38$ meV/Å^2 and $\gamma_{111} = 27.76$ meV/Å^2. However, our EAM calculations show that these three shapes are competitive in energy over various parts of this size range.

In order to understand the roles of interface, strain, and edge energies in determining precipitate shapes, it is necessary to separate their respective contributions to the precipitate energy, $E_{\mathrm{precip}} = E_{\mathrm{inter}} + E_{\mathrm{strain}} + E_{\mathrm{edge}} + E_{\mathrm{vertex}}$. To be specific, we illustrate by presenting the calculations of the edge energy $\varepsilon_{111\text{-}111}$ for octahedral Pb precipitates inserted in octahedral Al voids.

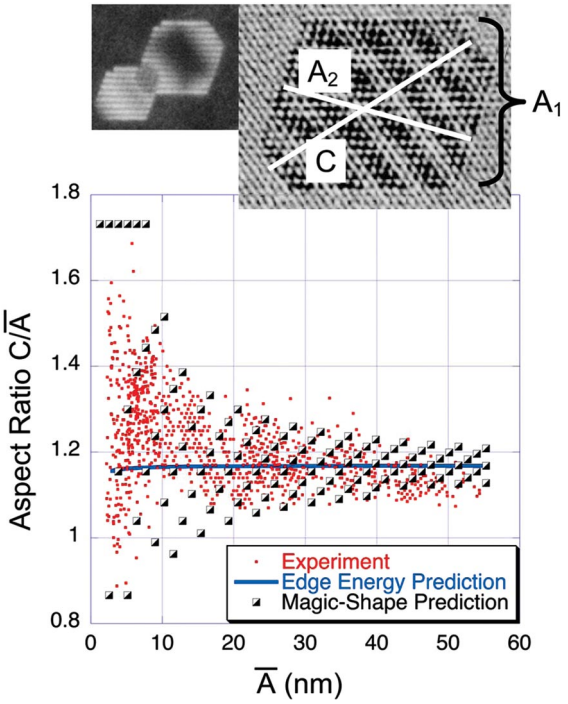

FIG. 1 (color). The upper right-hand inset shows a typical Pb precipitate in Al with the precipitate size defined as $\bar{A} = (A_1 + A_2)/2$. The red points show experimentally measured aspect ratios for a large experimental sample of such nanoprecipitates. The blue line shows the aspect ratio predicted by edge energies from the quantitative atomistic calculations described in the text. The square symbols plot the predictions of the magic-shape theory described in the text. The upper left inset shows two precipitates with a notch along one edge, also consistent with the magic-shape theory.

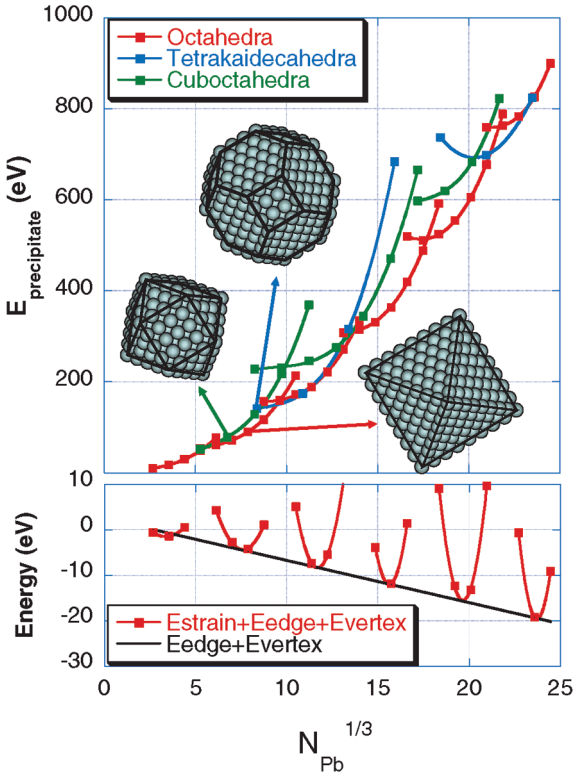

FIG. 2 (color). Summary of EAM calculations for Pb in Al. The upper plot shows E_{precip} as a function of the cube root of the number of Pb atoms in the precipitate. The insets show the three shapes considered: octahedra, tetrakaidecahedra, and cuboctahedra. The relative precipitate energies for these three shapes can be compared at a particular value of $N_{\text{Pb}}^{1/3}$ (corresponding to a given volume). The lower plot is constructed from the octahedra calculations by subtracting $E_{\text{inter}} = A_{111}\gamma_{111}$ from the precipitate energy, leaving $E_{\text{strain}} + E_{\text{edge}} + E_{\text{vertex}}$ (plotted as red points) and fit by a parabola for each value of Δ (see Table I). The minima of the parabolas represent the energies of zero-strain octahedral precipitates. The slope of the black line tangent to the parabolas gives the edge energy $\varepsilon_{111\text{-}111} = -19.5$ meV/Å.

We started with a block of approximately 10^5 Al atoms with periodic boundary conditions. Next an octahedron of Al atoms with n_{oct} atoms on each edge was removed. This void was filled by inserting an octahedron of Pb atoms with m_{oct} atoms on each edge. Because the lattice constants of Pb and Al are in the ratio $a_{\text{Pb}}/a_{\text{Al}} \approx 11/9$, only very small, elastic strains are generated if $n_{\text{oct}}/m_{\text{oct}} \approx 11/9$. The starting configurations are naturally categorized by the value of $\Delta = n_{\text{oct}} - m_{\text{oct}}$ as shown in Table I. For a given Δ, a small range of values for m_{oct} will correspond to precipitates with relatively small homogeneous strain. The total EAM energy E_{total} was determined by relaxing atomic positions using conjugate gradient energy minimization.

From E_{total}, the precipitate energy was obtained by subtracting the total cohesive energies, thus $E_{\text{precip}} = E_{\text{total}} - N_{\text{Al}}E_{\text{Al}} - N_{\text{Pb}}E_{\text{Pb}}$, where N_{Pb} is the number of Pb atoms in the precipitate, N_{Al} is the number of Al atoms in the Al matrix surrounding the precipitate, and E_{Al} and E_{Pb} are the bulk cohesive energies. The total number of atoms in the periodic simulation cell is $N_{\text{Al}} + N_{\text{Pb}}$. E_{precip} is plotted by the red points and fitted curves in the upper portion of Fig. 2.

The next step will be to calculate $E_{\text{precip}} - E_{\text{inter}} = E_{\text{strain}} + E_{\text{edge}} + E_{\text{vertex}}$. Before discussing the details of this calculation, we wish to point out that for the lowest strain precipitates, E_{precip} is less than E_{inter}, and thus $E_{\text{strain}} + E_{\text{edge}} + E_{\text{vertex}}$ is negative (as shown in the lower portion of Fig. 2). Since the strain energy can only be zero or positive, this implies that $E_{\text{edge}} + E_{\text{vertex}}$ is negative. The quantitative calculation of these quantities follows.

A previous publication [5] has described the calculation of edge energies for free Pd nanoclusters. A precise definition of edge length, based on the concept of the Gibbs equimolar dividing surfaces, was found to be absolutely essential in order to define and quantify the edge and vertex energies [10]. We use that definition to write

$$s_{\text{oct}} = \left[\sqrt[3]{m_{\text{oct}}^3 + \frac{m_{\text{oct}}}{2}}\right]\frac{a_{\text{Pb}}}{\sqrt{2}}.$$

Here s_{oct} is the edge length of the octahedron, m_{oct} is the

TABLE I. This table lists some of the octahedral precipitate configurations used for the EAM calculations. These configurations have relatively small homogeneous strain and correspond to the lowest strain points plotted in red in Fig. 2. Here, n_{oct} is the number of Al atoms on an edge of the removed Al octahedron and m_{oct} is the number of Pb atoms on an edge of the inserted Pb octahedron. These cases are selected to have small homogeneous elastic strains by choosing $n_{oct}/m_{oct} \approx a_{Pb}/a_{Al}$, and are grouped according to the value of $\Delta = n_{oct} - m_{oct}$.

$\Delta = 1$	$\Delta = 2$	$\Delta = 3$	$\Delta = 4$
$m_{oct} = 3$, $n_{oct} = 4$	$m_{oct} = 7$, $n_{oct} = 9$	$m_{oct} = 12$, $n_{oct} = 15$	$m_{oct} = 17$, $n_{oct} = 21$
$m_{oct} = 4$, $n_{oct} = 5$	$m_{oct} = 8$, $n_{oct} = 10$	$m_{oct} = 13$, $n_{oct} = 16$	$m_{oct} = 18$, $n_{oct} = 22$
$m_{oct} = 5$, $n_{oct} = 6$	$m_{oct} = 9$, $n_{oct} = 11$	$m_{oct} = 14$, $n_{oct} = 17$	$m_{oct} = 19$, $n_{oct} = 23$
	$m_{oct} = 10$, $n_{oct} = 12$	$m_{oct} = 15$, $n_{oct} = 18$	

number of atoms on an edge (including a vertex atom at each end), and a_{Pb} is the lattice constant of lead. The total area of an octahedron is $A_{111} = 2\sqrt{3}s_{oct}^2$. By subtracting the total interface energy, we find $E_{precip} - A_{111}\gamma_{111} = E_{strain} + E_{edge} + E_{vertex}$. This quantity is plotted in red in the lower portion of Fig. 2 for the Δ, n_{oct}, and m_{oct} values listed in Table I. Points for octahedra having $\Delta = 5$ or 6 are also plotted. These points are fit by parabolas since the strain energy for small homogeneous strains can be written as $E_{strain} = \alpha(s_{oct} - s_o)^2$ where s_o represents the octahedron edge length corresponding to zero elastic strain for a given value of Δ, and α is a constant for a given value of Δ. The strain energy can be estimated from analytical models for a spherical inclusion in a spherical void [7]. Curvatures of the parabolas plotting E_{strain} are in good agreement with that estimate.

To extract the edge energy, a tangent line was constructed to the parabolas having $\Delta = 2$, 3, 4, 5, and 6, as plotted in black in the lower section of Fig. 2. The slope of that tangent line gives the edge energy. This tangent line misses the minimum of the $\Delta = 1$ parabola, suggesting that the separation into edge and vertex energies is problematic for extremely small octahedra with 3, 4, or 5 Pb atoms on an edge. The edge energy calculated from the slope of the tangent line is $\varepsilon_{111\text{-}111} = -19.5$ meV/Å.

In order to calculate $\varepsilon_{111\text{-}111}$ we used the same procedure, but considered only cuboctahedral precipitates. For cuboctahedra, a different formula (see Ref. [5]) must be used to relate the edge length of a cuboctahedra s_{cub} to m_{cub}, the number of Pb atoms on an edge. The calculated edge energy is $\varepsilon_{111\text{-}100} = -19.2$ meV/Å. The two edge energies for Pb precipitates in Al are essentially equal.

We next consider the possible role of edge energy and interface energy based on the assumption that residual strains may be neglected. This is consistent with the observation that inclusions have nearly zero residual strain when they adopt magic-size dimensions [4]. For this case we write the energy of a truncated octahedral precipitate in the form $E = E_{inter} + E_{edge}$. To find the minimum energy for constant volume V, as a function of shape, we use Lagrange multipliers to minimize the function,

$$F = E/\gamma_{111} + \lambda V$$
$$= 2\sqrt{3}s^2 + 6(\rho - \sqrt{3})t^2 + 12\tau s + \lambda\sqrt{2}s^3/3 - \lambda\sqrt{2}t^3,$$

where s is the edge length of the untruncated octahedron, t is the truncation length, $\rho = \gamma_{100}/\gamma_{111}$, $\tau = \varepsilon/\gamma_{111}$, and $\varepsilon = \varepsilon_{111\text{-}111} = \varepsilon_{111\text{-}100} = -19.5$ meV/Å. Setting $\partial F/\partial t = \partial F/\partial s = 0$ and replacing the parameters t and s with appropriate combinations of the measured parameters C and $\bar{A}$, we obtain the aspect ratio as a function of size $\bar{A}$ as follows: $C/\bar{A} = (\rho + \sqrt{6}\tau/\bar{A})/(1 + \sqrt{2}\tau/\bar{A})$. This function (calculated using 400 K interfacial free energies) is plotted in Fig. 1 as a blue line. It is apparent from the plot that these edge energies have essentially no effect on the shape of Pb nanoprecipitates in Al. We have also confirmed that uncertainties in the edge energies on the order of $\varepsilon_{111\text{-}111} = \varepsilon_{111\text{-}100} \pm 5$ meV/Å will change the aspect ratio by only a very small amount. We also note that edge energy cannot explain the increasing scatter in aspect ratio observed for the smaller precipitates.

Since edge energy cannot be responsible for these effects, and they cannot be explained solely by interface energies (as in the Wulff construction), we turn our attention to strain energy, the only remaining possibility. In the following we consider how to construct a set of possible precipitate shapes having zero (or very small) homogeneous strain.

We start by observing that an fcc lattice can be built using two fundamental building blocks, a square pyramid (with one atom at each vertex) and a tetrahedron (also with one atom at each vertex). The rhombohedral primitive unit cell of the fcc lattice has one octahedral interstitial site and two tetrahedral interstitial sites, and can be constructed by placing two square pyramids base to base, forming an octahedron, and adding two tetrahedra placed on opposing triangular faces of this octahedron. If one wants to build strain-free fcc Pb precipitate nanoclusters in Al, it can only be done by assembling tetrahedral and square pyramid building blocks having 9 atoms on an edge. Such nanoclusters can be placed in a void created by removing the same Al shape having 11 atoms on an edge. In order to build these shapes with zero strain, the edge length of the tetrahedra and the square pyramids must be 9 times the Pb nearest neighbor distance or 31.5 Å. The concept of magic sizes, discussed in the literature [7], can be replaced by the criteria of magic shapes built from tetrahedra and square pyramids with edge length $s_{bb} = 31.5$ Å. For any shape constructed of these building blocks, the strain energy is

zero, and the interfacial energy can be calculated based on the interfacial areas, A_{111} and A_{100}, of the shape assembled from these building blocks.

In reality, we are interested not only in completely strain-free precipitates, but also in precipitates having very small homogeneous strains. Examples of such precipitates are listed in Table I in the columns labeled $\Delta = 1$ and $\Delta = 3$. To cover cases having odd as well as even integer values of Δ requires working with smaller structural building blocks having edge length $s_{bb} = 15.75$ Å. (The shapes with zero strain discussed in the previous paragraph can of course be assembled from these smaller building blocks.) The "magic shapes" are the set of possible precipitate shapes (and sizes) with zero or small strain, built with these building blocks with edge length $s_{bb} = 15.75$ Å.

We now have in hand the tools needed to explain the experimental data. In particular we have an algorithm to generate a set of precipitates with zero or small homogeneous strain. To illustrate, we consider precipitates with O_h symmetry, with shapes generated by starting with an octahedron with edge length s, and removing 6 square pyramids with edge length t. In order that the precipitates be nearly strain free, the concept of magic shapes requires that s must be quantized in units of $s_{bb} = 15.75$ Å, i.e., $s = ps_{bb}$ where p is a positive integer. Similarly, t must be quantized as $t = qs_{bb}$, where q is an integer $0 \leq q < p/2$.

Since these precipitates are nearly strain free, and since we have shown that edge energies make only a negligible contribution to shape effects, the precipitate energies are approximately equal to the interface energies, $E_{\text{precip}} \approx E_{\text{inter}} = A_{111}\gamma_{111} + A_{100}\gamma_{100}$. The aspect ratio is $C/A = (1 - t/s)\sqrt[3]{3}$, the total (100) area is $A_{100} = 6t^2$, and the total (111) area is $A_{111} = 8s^2 - 24t^2$. Here we use the $T = 400$ K interfacial free energies in order to predict the C/A ratio.

At this point, we know the aspect ratio and the interface energy of all the (nearly) stain-free precipitates with O_h symmetry. In order to predict the observed aspect ratios as a function of precipitate size, we need a criterion for deciding which precipitate energies might actually occur in a quasiequilibrium distribution of precipitates. For a given precipitate volume, it is easy to calculate the interfacial energy E_{Wulff} of a precipitate with the Wulff shape. Since this is the lowest possible energy for a given volume, we find it convenient to work with the energy $\Delta E = E_{\text{precip}} - E_{\text{Wulff}}$. For precipitates at equilibrium, one would expect a Boltzmann distribution of precipitate shapes with a characteristic $e^{-\Delta E/kT}$ probability. In this experiment, the precipitates are not at equilibrium and Ostwald ripening would continue slowly during further annealing. In order to reproduce the experimental shape distribution (shown as red points in Fig. 1), we rejected all precipitate sizes and shapes having $\Delta E > 60$ eV. While not rigorous, it appears that this energy criterion allows a shape distribution which, while far from equilibrium, is slowly ripening at the annealing temperature thereby avoiding shapes with very large ΔE. In Fig. 1 the black symbols represent the complete set of precipitate particles meeting four conditions: O_h symmetry, magic shape (i.e., near zero strain), $\Delta E \leq 60$ eV, and $\bar{A} \leq 55$ Å. The agreement between this magic-shape theory and the experimental data is seen to be good.

Finally we note that, in addition to the precipitates with O_h symmetry, there are many other precipitates which break this symmetry. In all cases, the experimentally observed shapes are consistent with the concept of magic shapes and nearly zero strain. The insets in Fig. 1 show two such cases where the symmetry is broken. In the upper right-hand inset the symmetry is broken because $A_1 \neq A_2$, while in the other inset the symmetry is broken by removing a row of tetrahedra and square pyramids to form a notch at an edge along the viewing direction.

To summarize, the model presented in this work accounts for the observed behavior of nanoscale solid inclusions. In particular, it is shown that while edge energy has a negligible effect on shape, strain energy leads to a sequence of magic shapes. The increasing granularity of such magic shapes at smaller sizes explains the increased scatter around the Wulff shape observed experimentally. We explain the experimental data by assembling magic shapes from building blocks which are tetrahedra and square pyramids with edge lengths $s_{bb} = 15.75$ Å. Given a set of magic shapes, we find that the members of this set with relatively small interface energies are the shapes that are observed. By providing an explanation for all the experimental data, our model offers an understanding of how nanoscale inclusions approach equilibrium under constraint within a solid matrix.

This work was supported by the U.S. Department of Energy, Basic Energy Sciences, Division of Materials Science, under Contract No. DE-AC04-94AL85000. Additional support was received from the Danish Natural Sciences Research Council.

[1] J. Nelson, Philos. Mag. A **81**, 2337 (2001).
[2] C. H. Nien and T. E. Mady, Surf. Sci. **380**, L527 (1997).
[3] O. E. Shklyaev, M. J. Beck, M. Asta, M. J. Miksis, and P. W. Voorhees, Phys. Rev. Lett. **94**, 176102 (2005).
[4] E. Johnson, A. Johansen, U. Dahmen, S. Chen, and T. Fujii, Mater. Sci. Eng. A **304–306**, 187 (2001).
[5] J. C. Hamilton, Phys. Rev. B **73**, 125447 (2006).
[6] C. M. Retford, M. Asta, M. J. Miksis, P. W. Voorhees, and E. B. Webb, Phys. Rev. B **75**, 075311 (2007).
[7] U. Dahmen, S. Q. Xiao, S. Paciornik, E. Johnson, and A. Johansen, Phys. Rev. Lett. **78**, 471 (1997).
[8] A. Landa, P. Wynblatt, D. J. Siegel, J. B. Adams, O. N. Mryasov, and X. Y. Liu, Acta Mater. **48**, 1753 (2000).
[9] A. Landa, P. Wynblatt, E. Johnson, and U. Dahmen Acta Mater. **48**, 2557 (2000).
[10] The requirement for precise definition of interface surfaces was mentioned briefly in C. Rottman and M. Wortis, Phys. Rep. **103**, 59 (1984).